TASR Trends in Applied Sciences Research

OPEN ACCESS

Molecular Structure, Vibrational and Antibacterial Activity Studies on Mono 4-Sulfamoylanilinium Citrate Crystal

C. Muthuselvi, P. Bhuvaneswari and C. Dhivya Bharathi
Department of Physics, Devanga Arts College, Aruppukottai 626101, Tamil Nadu, India

ABSTRACT

Background and Objective: Sulfa drugs were mostly prescribed as chemotherapeutic agents for the treatment of infectious diseases. The structural modifications were preferred due to reducing the toxicity effect of the drug molecule. Many studies had been encountered on the synthesis of sulfanilamide derivative complex crystal. In this manner, the present work was carried out to grow the mono 4-sulfamoylanilinium citrate (M4-SAC) complex crystal in an organic-inorganic hybrid. **Materials and Methods:** Sulfanilamide, citric acid, distilled water and ethanol was used in this crystallization process. The single crystals were harvested from the slow evaporation method at room temperature. **Results:** The 3D molecular structure was computed using Chem3D software. The obtained crystal was analyzed by powder X-ray diffraction, FT-IR, FT-Raman, Optical, SEM with EDX and antimicrobial activity studies. **Conclusion:** The crystal structure of the M4-SAC compound had a sulfamoylanilium cation and a citrate anion which were interlinked through the N–H...O hydrogen bond. To elucidate the crystalline nature of the material, a powder XRD study can be used. The various functional groups present in the title crystal were assigned using IR and Raman spectroscopic techniques. The optical band gap was determined as 3.9 eV. The SEM with EDX study confirms the formation of the M4-SAC complex crystal. The antimicrobial activity study reveals that the complex crystal enhanced the inhibition zone against *Bacillus subtilis* and *Acinetobacter baumannii* bacteria.

KEYWORDS

PXRD, IR, Raman, UV-visible, SEM with EDX, antibacterial

INTRODUCTION

The organic compound of sulfanilamide is an aniline derivative with a sulfonamide group in which the sulfamoyl functional group is attached to aniline at the 4th position[1,2]. The IUPAC name of sulfanilamide is 4-aminobenzenesulfonamide, which is a white crystal powder[3]. It is the most common type of antibiotic to treat infectious diseases in humans and animals. Also, it performs bacteriostatic activity against many gram-negative and gram-positive organisms[4]. The sulfanilamide drugs are widely used as effective chemotherapeutic agents to prevent bacterial infections in humans and they also are employed as antifungal, antitumor, anhydrase inhibitors, antiviral and anti-inflammatory agents[5-10]. But due to the toxicity, it is rarely used as a systemic drug. However, today sulfanilamide remains used in the treatment

ISSN: 2151-7908 (Online)
ISSN: 1819-3579 (Print)
https://doi.org/10.3923/tasr.2022.157.167

Received: 25 Apr. 2022
Accepted: 10 Aug. 2022
Published: 01 Oct. 2022

of vaginal yeast infections caused by candida albicans[11]. The sulfanilamide derivatives exhibit high inhibitory activities against bacteria, yeasts and fungi. Many previous studies concerning the structure of sulfanilamide derivative crystals with different inorganic acid combinations have been reported by Zgolli *et al.*[12], Ravikumar *et al.*[13], Pandiarajan *et al.*[14], Anitha *et al.*[15], Muthuselvi *et al.*[16] and Muthuselvi *et al.*[17]. The structure-activity relationship of the substituted sulfanilamides has been subjected to many studies. Based on the above specifics, an investigation of sulfanilamide reactivity with organic acid was undertaken in the present study. Taking into account, an attempt was made to grow the novel sulfanilamide complex crystal with organic acid by the slow evaporation method. Using Chem 3D software, the molecular structure of the title compound was obtained by the MM2 method. This frame was aimed at the synthesis of mono 4-sulfamoylanilinium citrate (M4-SAC) crystal and which has been characterized using powder XRD, FT-IR, FT-Raman, UV-Visible-NIR spectroscopy, SEM with EDX and antibacterial activity studies in this work.

MATERIALS AND METHODS

Study area: In December 2021, the title crystal was grown at the Research Department of Physics, Devanga Arts College, Aruppukottai, Tamil Nadu, India. The data were collected between January and March, 2022.

Chemical used: Sulfanilamide at >98% and citric acid at >99.5% were purchased from Sigma Aldrich Company. The ethanol and distilled water solvents were obtained from Modern Scientific Company, a Laboratory equipment supplier in Madurai, Tamil Nadu.

Computational details: The 3D molecular structure of the M4-SAC crystal was computed by Molecular Mechanics (MM2) method in the Chem3D desktop modelling program under gas-phase conditions.

Methods: Crystals of mono 4-sulfamoylanilium citrate were made by mixing the aqueous ethanol solution of sulfanilamide and the aqueous solution of citric acid in the stoichiometric ratio of 1:1 at room temperature. The stirred solution was filtered by filter paper and placed in the petri dish. After 20 days duration, brown-colored crystals were obtained by the slow evaporation process. The harvested crystal photograph and chemical structure of the M4-SAC crystal is shown in Fig. 1 and 2, respectively.

Fig. 1: Grown crystal of M4-SAC

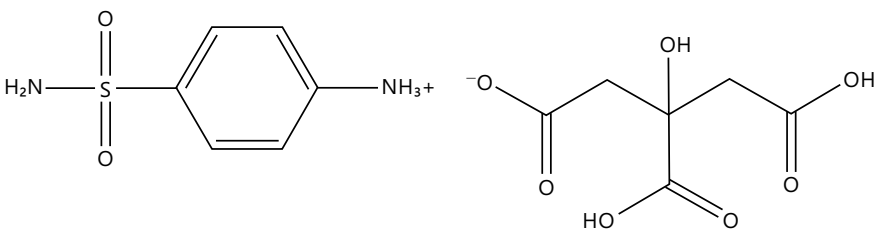

Fig. 2: Chemical structure of M4-SAC crystal

Experimental details: The powder X-ray diffraction analysis was performed by XPERT-PRO X-ray diffractometer with Cu Kα radiation (1.54060Å) in the 2θ range 20°-80° at Alagappa University, Karaikudi. The FT-IR spectrum was obtained using a SHIMADZU FT-IR spectrometer in the wavenumber range 400-4000 cm^{-1} with a KBr disc at V.H.N.S.N. College, Virudhunagar. The FT-Raman spectrum was made with BRUKER: RFS 27 Raman spectrometer in the wavenumber range 4000–400 cm^{-1} at SAIF, IIT Madras. The optical absorption spectrum had been recorded with SHIMADZU-UV 1601, a double beam spectrometer in the wavelength range 190-1100 nm at V.H.N.S.N. College, Virudhunagar. The SEM and elemental analysis were performed using CARL ZEISS EVO18 scanning electron microscope at Kalasalingam University, International Research Centre, Krishnankoil, Tamil Nadu, India. In Sri Kaliswari College, Sivakasi, Tamilnadu, India, the antimicrobial activity study was performed by agar well diffusion method in Mueller Hinton Agar (MHA) plates with DMSO as a positive control.

RESULTS AND DISCUSSION

3D-molecular structure analysis: Figure 3 shows the molecular structure of the M4-SAC crystal which was obtained with the steric energy-195.46 kcal mol^{-1} using Chem 3D and ChemDraw professional software (version 16.0). The title compound contains a cation with a protonated amino group and a citrate anion. The transfer of a proton (H-atom) from the citric acid leads to the protonation in the 4-sulfanilamide and forms a 4-sulfamoylanilinium cation. In the molecular structure, the sulfamoylanilium cation was interlinked with citrate anion through the formation of a N_a-H···O (a = aniline) hydrogen bond. The molecular formula of the title compound was $C_{12}H_{16}N_2O_9S$ and its molecular weight was 364.33 g moL^{-1}.

Powder X-ray diffraction analysis: Due to the low transparency of the grown title crystal, were not able to perform the single crystal XRD analysis. However, the PXRD study can be reduced this difficulty with this kind of material. The experimentally recorded powder XRD pattern has sharp intense peaks which were due to every substance in the grown crystal producing its diffraction pattern in Fig. 4. Also, it reveals the good crystalline nature and purity of the M4-SAC crystal. The experimentally obtained 2θ and d-spacing values of M4-SAC crystal were compared with standard values of their parent compounds i.e., sulfanilamide (JCPDS card No. 63-74-1) and citric acid (JCPDS card No. 77-92-9). The results show that experimental values do not match the standard values of their parent compounds and this analysis confirms that the M4-SAC crystal was fashioned in complex form. The average microcrystalline size and dislocation density was determined using the formulas described in earlier literature by Mhadhbi *et al.*[18] and Abolghasem *et al.*[19]. The average crystalline size and dislocation density was determined as 81 nm and 1.56×10^{14} m^2, respectively for the title crystal.

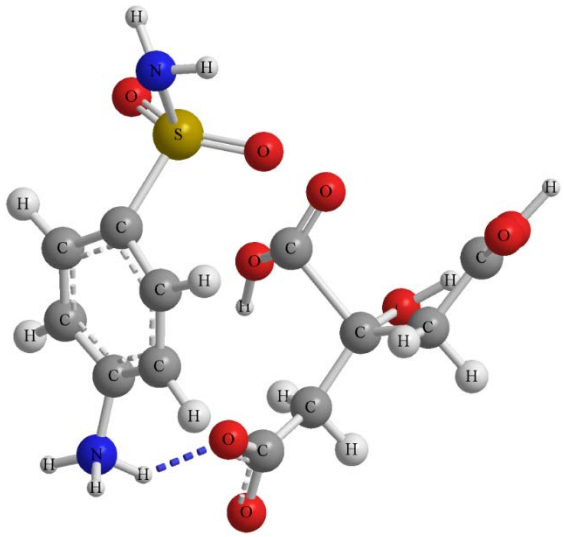

Fig. 3: 3D molecular structure of M4-SAC crystal, a hydrogen bond is shown as the dashed line

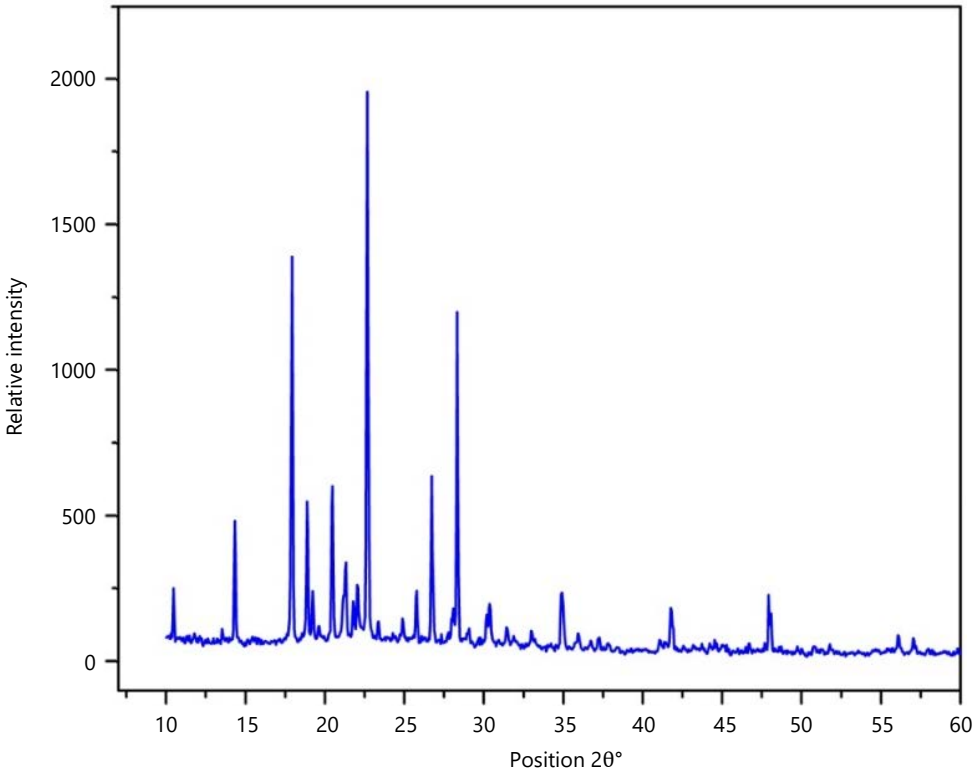

Fig. 4: Powder X-ray diffraction pattern for M4-SAC crystal

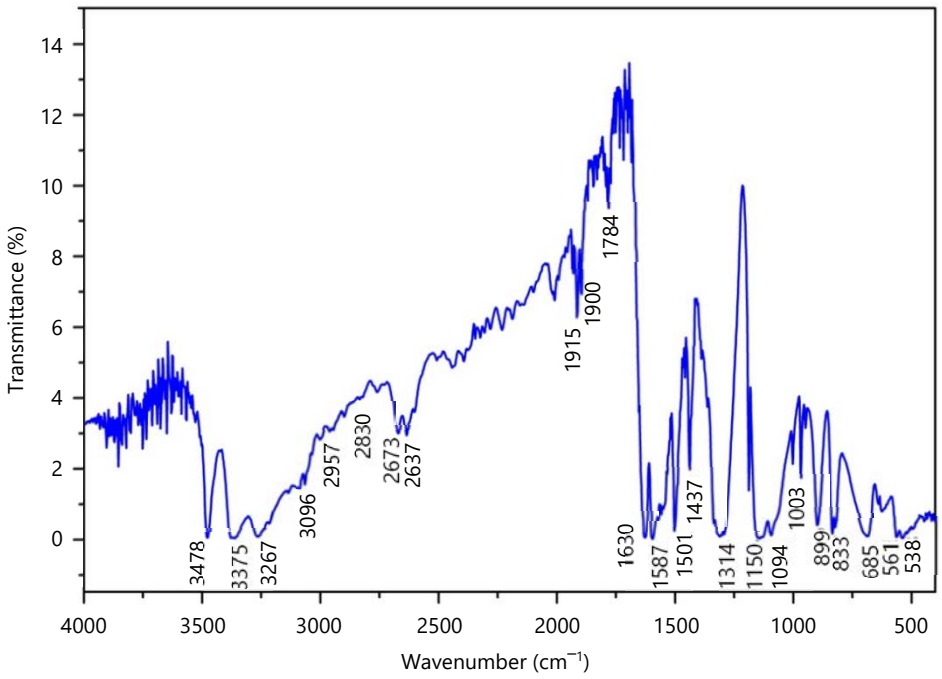

Fig. 5: FT-IR spectrum of M4-SAC crystal

FT-IR and FT-Raman spectral analysis: The experimentally recorded FT-IR and FT-Raman spectra are illustrated in Fig. 5 and 6, respectively. In the present work, the normal modes of vibration of 4-sulfamoylanilinium cation and citrate anion were investigated via the experimentally recorded IR and Raman spectra. M4-SAC crystal has -$[NH_3]^+$, -NH_2, -SO_2, C-N, C-S, C-H, C-C, C=C, -CH_2, C-O, C=O and O-H functional groups. The characteristic wavenumbers for these functional groups were identified and assigned in Table 1.

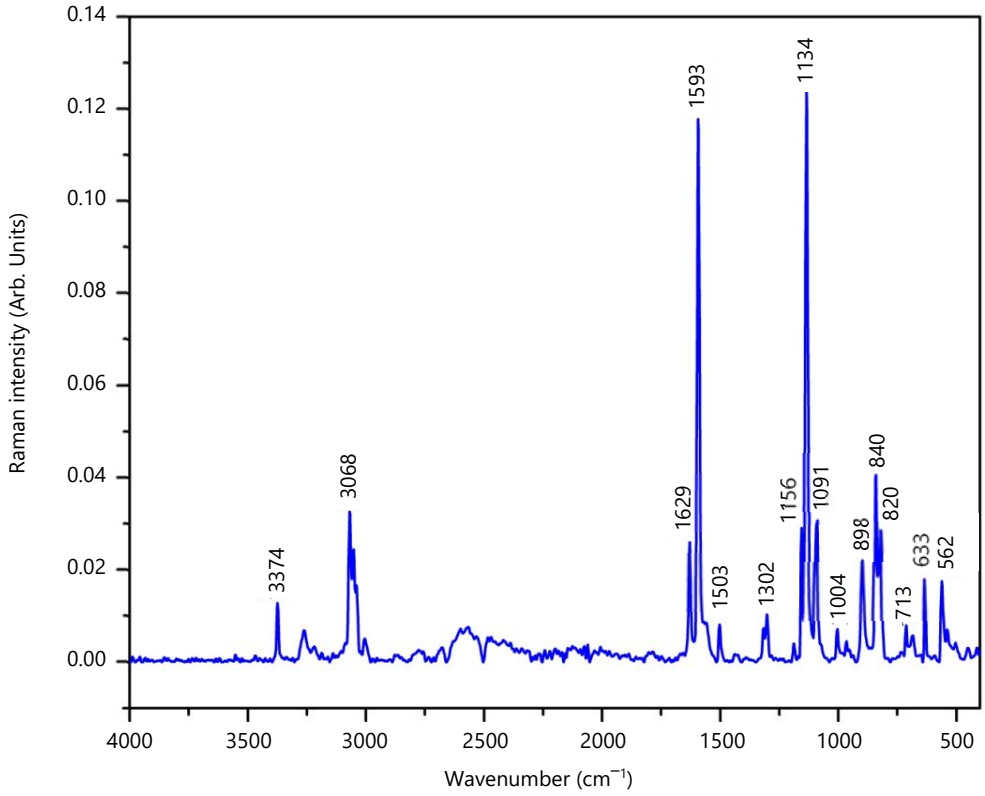

Fig. 6: FT-Raman spectrum of M4-SAC crystal

Sulfamoylanilinium cation residue

Vibrations of -[NH_3]$^+$ group: The -[NH_3]$^+$ antisymmetric and symmetric stretching vibrations were observed at 3140 and 2830 cm^{-1} in the IR spectrum. But in the Raman spectrum, there was no counterpart for these modes. The scissoring mode of the -[NH_3]$^+$ group was identified as a shoulder peak at 1545 cm^{-1} in the IR spectrum whereas, the corresponding Raman line was absent. The rocking vibration falls at 1142 cm^{-1} in IR and 1136 cm^{-1} in Raman spectra. The twisting vibrations were observed as strong bands at 561 and 538 cm^{-1} in the FT-IR spectrum and also the wagging mode was attributed as medium peaks at 968 and 947 cm^{-1} in the FT-IR spectra. These wavenumber assignments were in good agreement with the earlier reports of related compounds[20,21].

Vibrations of -NH_2, -SO_2, C-S and C-N groups: The IR band corresponding to antisymmetric and symmetric stretching modes of -NH_2 belonging to the sulfonamide group was observed at 3375 cm^{-1} and 3267 cm^{-1}, respectively. In this study, the scissoring, rocking and wagging modes of the -NH_2 group were observed at 1630 cm^{-1} (IR), 1437 cm^{-1} (IR) and 685 cm^{-1} (IR), respectively. The peaks recorded at 1337 cm^{-1} in the Raman spectrum and 1150 cm^{-1} in the IR spectrum were assigned to $\nu_{as}(SO_2)$ and $\nu_s(SO_2)$ mode, respectively. The scissoring and wagging modes of the SO_2 group were assigned in the region 621 and 561 cm^{-1}, respectively. The title crystal exhibits a medium intensity band in both spectra at 899 and 897 cm^{-1} for the stretching mode of S-N vibration. The C-N stretching mode was assigned at 1314 cm^{-1} in the IR spectrum only. The C-S stretching mode occurs at 621 and 639 cm^{-1} in the infrared and Raman spectra, respectively. All the above functional group vibrations exactly matched the previously reported values[22].

Vibrations of the para-substituted benzene ring: The C-H stretching vibration of distributed benzenes had been assigned at 3096, 3067 and 3003 cm^{-1} in FT-IR and 3084, 3015 cm^{-1} in FT-Raman spectra. The β(C-H) mode was observed at 1314 and 1184 cm^{-1} infrared spectrum and the out-of-plane C-H deformation bands were observed at 968 and 947 cm^{-1} in the FT-IR spectrum. The C-C and C=C stretching

Table 1: Wavenumber assignments for M4-SAC crystal in FT-IR and FT-Raman spectra

FT-IR ($\bar{\nu}$ cm^{-1})	FT-Raman ($\bar{\nu}$ cm^{-1})	Assignment
3478 (s,)	-	$\nu(O\text{-}H)_{water}$
3375 (s)	-	$\nu_{as}(\text{-}NH_2)_{amide}$
3370 (s)	-	$\nu_{as}(\text{-}NH_2)_{amide}$
3267 (s)	-	$\nu_{s}(\text{-}NH_2)_{amide}$
3140 (sh)	-	$\nu_{as}(\text{-}NH_3)^+$
3096 (m)	3084 (s)	$\nu(C\text{-}H)$, $\nu(\text{-}OH)_{acid}$
3067 (m)	-	$\nu(C\text{-}H)$
3003 (w)	3015 (w)	$\nu(C\text{-}H)$
2957 (w)	2985 (m)	$\nu_{as}(\text{-}CH_2)$
2830 (w)	-	$\nu_{s}(\text{-}NH_3)^+$, $\nu_{s}(\text{-}CH_2)$
1960 (w) 1890 (w) 1844 (w) 1825 (w)	-	Overtone/combination bands
1784 (w)	-	$\nu(C{=}O)_{acid}$
-	1714 (m)	$\nu(C{=}O)_{acid}$
1630 (s)	-	$\nu(C\text{-}C)$, $\rho(NH_2)_{amide}$, $\delta(O\text{-}H)_{water}$
1622 (sh)	-	$\nu(C\text{-}C)$
1587 (s)	-	$\nu(C\text{-}C)$, $\nu_{as}(COO^-)$
1545 (sh)	-	$\rho(\text{-}NH_3)^+$
1501 (s)	-	$\rho(CH_2)$
1437 (m)	-	$\tau(NH_2)_{amide}$, $\nu(C{=}C)$
-	1337 (m)	$\nu_{s}(COO^-)$, $\nu_{as}(\text{-}SO_2)$, $\omega(\text{-}CH_2)$
1314 (s, br)	-	$\nu(C\text{-}N)$, $\beta(C\text{-}H)$
-	1252 (m)	$t(\text{-}CH_2)$, $\nu(C\text{-}O)$
-	1210 (m)	$\nu(C\text{-}O)$
1184 (sh)	-	$\beta(C\text{-}H)$, $\nu(C\text{-}C\text{-}O)$
1150 (s, br)	-	$\nu_{s}(\text{-}SO_2)$
1142 (s, br)	1136 (w)	$\tau(\text{-}NH_3)^+$
968 (m)	-	$\gamma(C\text{-}H)$, $\omega(O\text{-}H)$, $\omega(\text{-}NH_3)^+$
947 (w)	-	$\gamma(C\text{-}H)$
899 (m)	897 (m)	$\nu(S\text{-}N)$
833 (s)	835 (s)	Benzene ring breathing mode
685 (s, br)	-	$\omega(\text{-}NH_2)$, $\delta(CO_2)$, $t(O\text{-}H)$, $\rho(O\text{-}C{=}O)$, $\rho(COO^-)$
621 (s, br)	639 (m)	$\rho(\text{-}SO_2)$, $\delta(CO_2)$, $t(O\text{-}H)$, $\nu(C\text{-}S)$
561 (s)	-	$\omega(\text{-}SO_2)$, $t(O\text{-}H)$, $\omega(O\text{-}C{=}O)$, $\omega(COO^-)$, $t(\text{-}NH_3)^+$
538 (s)	-	$\tau(CO_2)$, $\tau(O\text{-}C{=}O)$, $\tau(\text{-}NH_3)^+$
447 (m)	-	$\tau\ (COO^-)$

s: Strong, m: Medium, w: Weak, sh: Shoulder, u: Stretching, u_s: Symmetric stretching, u_{as}: Anti symmetric stretching, δ: Bending, β: In-plane bending, γ: Out-of-plane bending, ρ: Scissoring, t: Twisting, ω: Wagging and τ: Rocking

vibrations were attributed at 1630, 1622, 1587 and 1437 cm^{-1}, respectively in the infrared spectrum. The ring breathing mode for para-substituted benzene ring was observed at 833 cm^{-1} in FT-IR and 835 cm^{-1} in FT-Raman spectra[23].

Citrate anion residue

Vibrations of the -CH_2 group: The ν_{as} (-CH_2) mode was assigned at 2957 cm^{-1} (IR) and 2985 cm^{-1} (Raman) and ν_s(-CH_2) was attributed at 2830 cm^{-1} in the IR spectrum for the title crystal. The bands attributed at 1501 cm^{-1} in IR and 1337, 1252 cm^{-1} in Raman spectra were assigned to the scissoring, wagging and twisting modes of the -CH_2 group.

Vibrations of carboxyl group: The vibrations observed at 3096, 3067 cm^{-1} in IR and at 3084 cm^{-1} in Raman spectra were assigned to the O-H stretching vibration of the CO-OH group. The C-O stretching of carboxylic acid was identified at 1252 cm^{-1} and 1210 cm^{-1} in the Raman spectrum. The IR peak arises at 1184 cm^{-1} for the C-C-O stretching mode. The absorption band at 1784 and 1714 cm^{-1} were assigned

to C=O stretching mode. The spectrum has a strong band at 538 cm^{-1} due to the rocking vibration of the

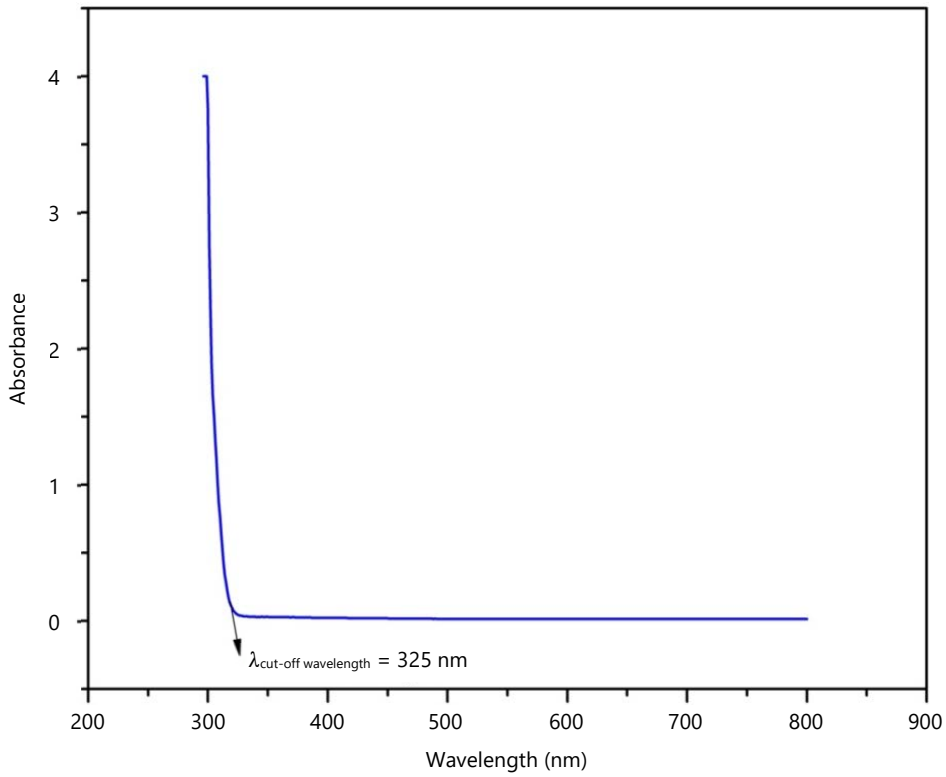

Fig. 7: Absorbance spectrum for M4-SAC crystal

CO_2 group. Also, the bending vibrations of the CO_2 group result in a band at 685, 621 cm^{-1} in IR and 639 cm^{-1} in Raman spectra. The out-of-plane wagging mode of the O-H group should be expected at 968 cm^{-1} and the twisting mode was predictable at 685, 621 and 561 cm^{-1} in the IR spectrum. The bands recognized at 685, 561, 538 cm^{-1} in FT-IR and at 639 cm^{-1} in Raman spectra had been assigned to the scissoring, wagging and rocking modes of the O-C=O group, respectively[22].

Vibration of COO^- group: The vibration was identified at 1587 cm^{-1} in IR for the antisymmetric mode of the COO^- group. Also, the symmetric stretching mode for the same group was identified at 1337 cm^{-1} in the Raman spectrum. The scissoring, wagging and rocking deformation modes were recorded at 685, 621 and 447 cm^{-1}, respectively. All these wavenumber assignments were exactly coincidental with the recently reported values[24].

Vibrations of H_2O molecule: The strong peak 3431 cm^{-1} in the IR spectrum was assigned to the symmetric stretching mode of water during KBr pellet preparation. The bending mode was attributed as a medium band at 1630 cm^{-1} in the FT-IR spectrum[23].

Optical band gap analysis: The UV-Visible absorbance spectrum and optical band gap graph are shown in Fig. 7 and 8, respectively. The optical band gap was determined using Tauc's plot. The plot was drawn between $(\alpha h\nu)^2$ Vs photon energy ($h\nu$). The extrapolation of the linear part of $(\alpha h\nu)^2$ to the photon energy axis directly gives the optical band gap, it was established at 3.9 eV. The lower cut-off wavelength was found at 325 nm and the grown crystal had large transmittance in the entire visible region.

Surface morphology and elemental analysis: The SEM images with 500x and 2.5kx magnifications of the M4-SAC compound were taken with an acceleration voltage of 20 kV which is shown in Fig. 9a and b, respectively. The images reveal the homogeneity nature of the sample. To confirm the formation of mono 4-sulfamoylanilinium citrate complex crystal, the EDX analysis was performed. The EDX spectrum is shown in Fig. 10, the x-axis is energy in keV and the y-axis is counts. The presence of C, N, O and S elements in the EDX spectrum confirms the formation of the M4-SAC complex crystal.

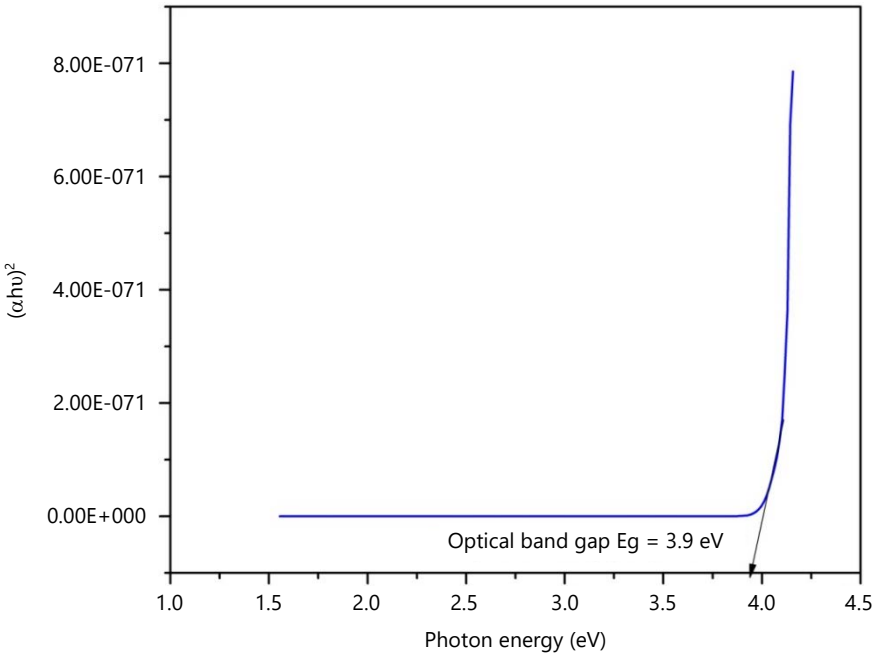

Fig. 8: Optical band gap for M4-SAC crystal

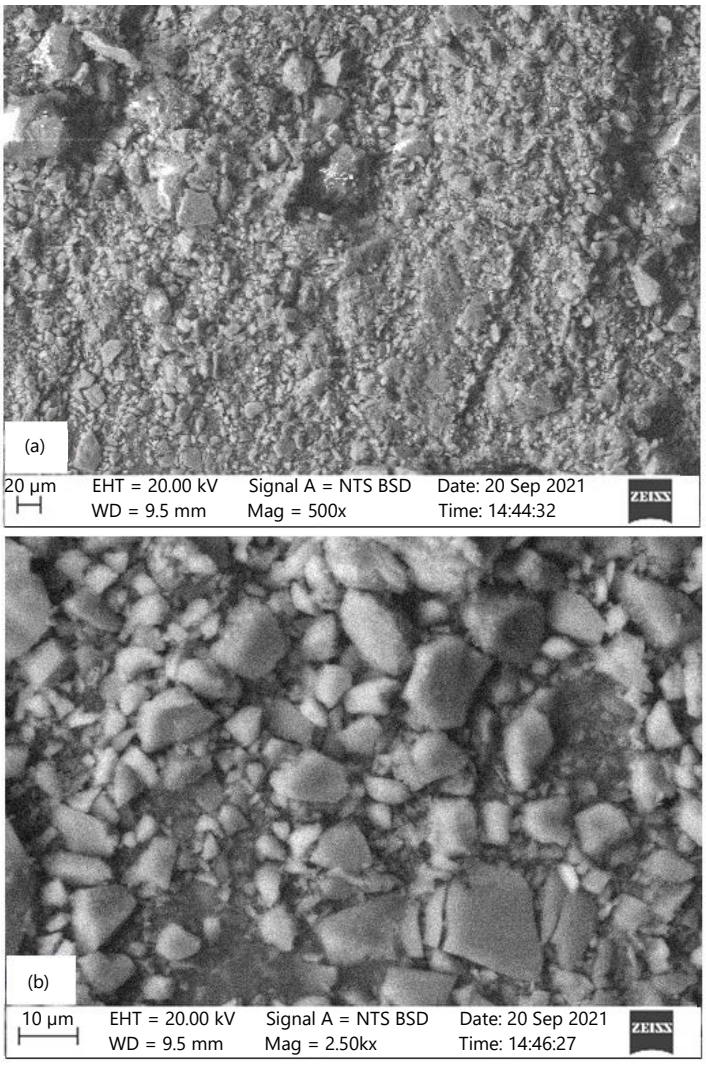

Fig. 9: SEM images of M4-SAC crystal with (a) 500X and (b) 2.5 kX magnifications

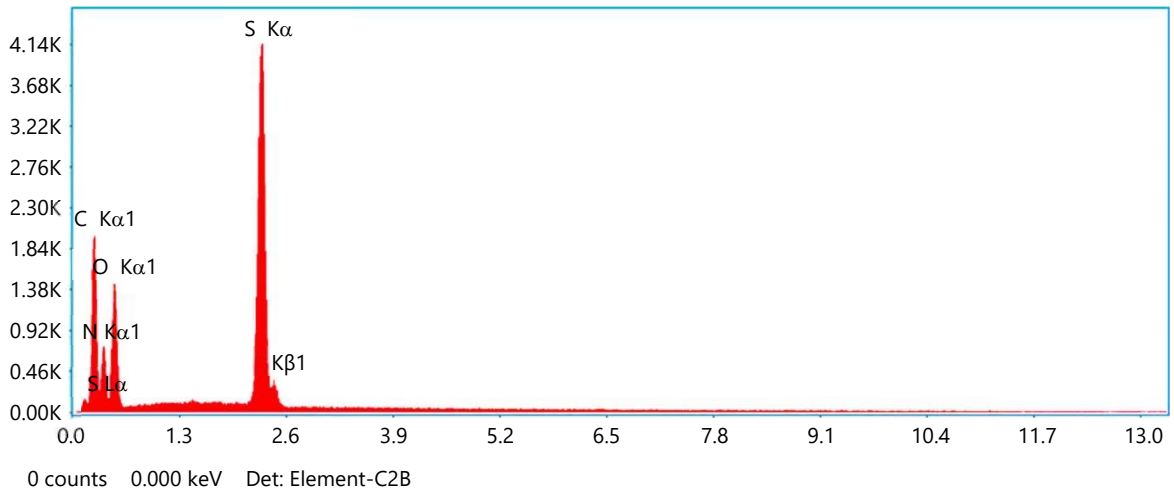

Fig. 10: EDX spectrum of M4-SAC crystal

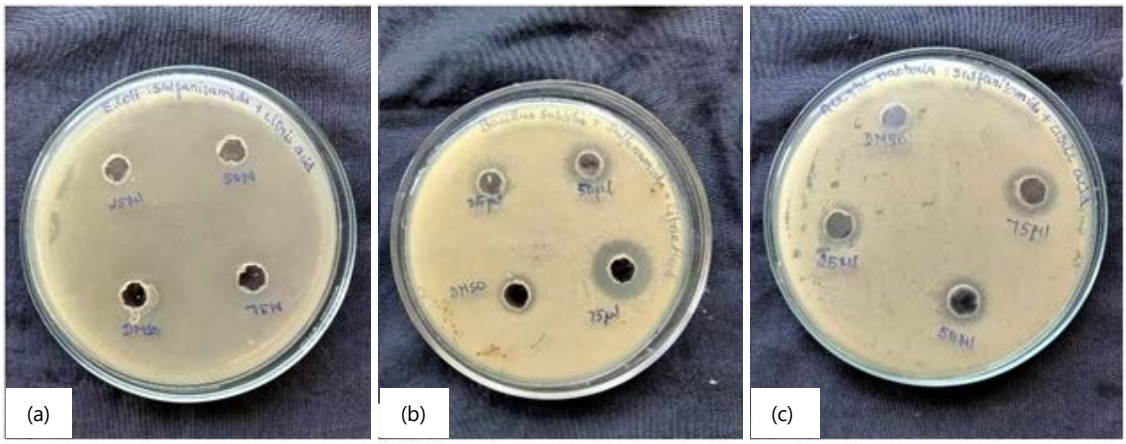

Fig. 11(a-c): Photographic view showing inhibition region of M4-SAC crystal against bacterial species at 25, 50 and 100 µg L^{-1} concentrations, (a) *Escherichia coli*, (b) *Bacillus subtilis* and (c) *Acinetobacter baumannii* bacteria

Table 2: Diameter of zones of inhibition (mm) for M4-SAC crystal against microorganisms

	Plant extract concentration (µg mL^{-1})		
Bacteria (B)	25	50	75
Escherichia coli	NZ*	NZ*	NZ*
Bacillus subtilis	3 mm	5 mm	7 mm
Acinetobacter baumannii	4 mm	5 mm	7 mm

*NZ: No zone of inhibition

Antibacterial activity analysis: A total of 3 human pathogenic microbial strains were used in the study: *Escherichia coli*, *Bacillus subtilis* and *Acinetobacter baumannii*. Antimicrobial assay of extracts of different plants was performed by agar well diffusion method in Mueller Hinton Agar (MHA) plates. Plant extracts of 50 mg/ml concentration were prepared in Dimethyl Sulfoxide (DMSO). Three wells of 6 mm were bored in the inoculated media with the help of a sterile cork borer (6 mm). Each well was filled with 25, 50 and 75 µL, extracts from different plant extract concentrations: Positive control (DMSO). It was allowed to diffuse for about 30 min at room temperature and incubated for 18-24 hrs at 37°C. After incubation, plates were observed for the formation of a clear zone around the well which corresponds to the antimicrobial activity of tested compounds in Fig. 11a-c. The Zone of Inhibition (ZOI) was observed and measured in mm. The M4-SAC compound had shown high antibacterial activities against *Bacillus subtilis* and *Acinetobacter baumannii* bacteria with diameter inhibition ranging from 3-7 mm. But it had no

antibacterial activity on *Escherichia coli* bacteria. The results are reported in Table 2.

CONCLUSION

The mono 4-sulfamoylanilium citrate crystal was crystallized using the slow evaporation technique at room temperature. The 3D molecular structure was performed and visualized by Chem3D and ChemDraw Professional software. Due to the low transparency of the crystal, the crystallite nature was analyzed using a powder XRD study. The appearance of strong intensity peaks of complex crystals was shifted from their parent compounds. The FT-IR and FT-Raman spectra of the M4-SAC crystal were studied. The presence of various functional group vibrations in the IR and Raman spectrum had been assigned and compared with the already reported literature values. The optical band gap was determined as 3.9 eV using Tauc's plot. The surface morphology and elemental analysis confirmed the formation of the M4-SAC complex crystal. The complex M4-SAC crystal had high antimicrobial activity against *Bacillus subtilis* and *Acinetobacter baumannii* bacteria.

SIGNIFICANCE STATEMENT

This study realizes the synthesis of a new organic-organic hybrid that can play a widespread role in medicinal chemistry. This study will help the researcher discover a new sulfanilamide derivative complex crystal. To improve the high inhibitory activities against the bacteria, yeasts and fungi, an attempt was made to grow the organic-organic complex crystal using the slow evaporation method.

ACKNOWLEDGMENT

The authors sincerely acknowledge their gratitude to the Management and Principal of Devanga Arts College, Aruppukottai, Tamilnadu, India for their consent and support during their research work.

REFERENCES

1. Borba, A., A. Gómez-Zavaglia and R. Fausto, 2013. Conformational landscape, photochemistry, and infrared spectra of sulfanilamide. J. Phys. Chem., 117: 704-717.
2. Zevzikoviene, A., A. Zevzikovas, E. Tarasevicius, A. Pavlonis and V. Dirse, 2012. Synthesis and *in vitro* antimicrobial study of 4-thiazolidinone containing sulfanilamide. Acta Poloniae Pharm., 69: 911-915.
3. Granger, S. and H. Iizumi, 2001. Water Quality Measurement Methods for Seagrass Habitat. In: Global Seagrass Research Methods, Short, F.T. and R.G. Coles (Eds.), Elsevier Science, Amsterdam, ISBN: 978-0-444-50891-1, pp: 393-406.
4. Essghaier, B., A. Naouar, J. Abdelhak, M.F. Zid and N. Sadfi-Zouaoui, 2014. Synthesis, crystal structure and potential antimicrobial activities of di (4-sulfamoyl-phenyl-ammonium) sulphate. Microbiol. Res., 169: 504-510.
5. Ajibade, P.A., G.A. Kolawole, P. O'Brien, M. Helliwell and J. Raftery, 2006. Cobalt(II) complexes of the antibiotic sulfadiazine, the X-ray single crystal structure of $[Co(C_{10}H_9N_4O_2S)_2(CH_3OH)_2]$. Inorg. Chim. Acta, 359: 3111-3116.
6. Isik, S., F. Kockar, M. Aydin, O. Arslan and O.O. Guler *et al*., 2009. Carbonic anhydrase inhibitors: Inhibition of the β-class enzyme from the yeast *Saccharomyces cerevisiae* with sulfonamides and sulfamates. Bioorg. Med. Chem., 17: 1158-1163.
7. Bouissane, L., S. El Kazzouli, S. Léonce, B. Pfeiffer, E.M. Rakib, M. Khouili and G. Guillaumet, 2006. Synthesis and biological evaluation of *N*-(7-indazolyl)benzenesulfonamide derivatives as potent cell cycle inhibitors. Bioorg. Med. Chem., 14: 1078-1088.
8. Ovung, A. and J. Bhattacharyya, 2021. Sulfonamide drugs: Structure, antibacterial property, toxicity, and biophysical interactions. Biophys. Rev., 13: 259-272.
9. Gawin, R., E. de Clercq, L. Naesens and M. Koszytkowska-Stawińska, 2008. Synthesis and antiviral evaluation of acyclic azanucleosides developed from sulfanilamide as a lead structure. Bioorg. Med. Chem., 16: 8379-8389.
10. Weber, A., A. Casini, A. Heine, D. Kuhn, C.T. Supuran, A. Scozzafava and G. Klebe, 2004. Unexpected nanomolar inhibition of carbonic anhydrase by COX-2-selective celecoxib: New pharmacological opportunities due to related binding site recognition. J. Med. Chem., 47: 550-557.

11. Scholar, E., 2007. Sulfanilamide. In: xPharm: The Comprehensive Pharmacology Reference, Enna, S.J. and D.B. Bylund (Eds.), Elsevier, Amsterdam, ISBN: 978-0-08-055232-3, pp: 1-5.
12. Zgolli, D.Z., H. Boughzala and A. Driss, 2010. 4-sulfamoylanilinium chloride. Acta Crystallogr. Sec. E: Crystallogr. Commun., Vol. E66. 10.1107/s1600536810019471.
13. Ravikumar, B., S. Pandiarajan and S. Athimoolam, 2013. Bis(4-sulfamoylanilinium) sulfate. Acta Crystallogr. Sec. E: Crystallogr. Commun., Vol. E69. 10.1107/s1600536813007216.
14. Pandiarajan, S., S. Balasubramanian, B. Ravikumar and S. Athimoolam, 2011. 4-sulfamoylanilinium nitrate. Acta Crystallogr. Sec. E: Crystallogr. Commun., Vol. E67. 10.1107/s1600536811038827
15. Anitha, R., S. Athimoolam, M. Gunasekaran and B. Sridhar, 2013. 4-sulfamoylanilinium perchlorate. Acta Crystallogr. Sec. E: Crystallogr. Commun., Vol. E69. 10.1107/s1600536813017972
16. Muthuselvi, C., N. Mala, N. Srinivasan, S. Pandiarajan and R.V. Krishnakumar, 2014. Crystal structure of 4-sulfamoylanilinium dihydrogen phosphate. Acta Crystallogr. Sec. E: Crystallogr. Commun., E70: o997-o998.
17. Muthuselvi, C., S. Pandiarajan, S. Athimoolam, R.V. Krishnakumar and A. Manikandan, 2017. Structural and optical properties of NLO material: 4-sulfamoylanilinium dihydrogen phosphate. Adv. Sci. Eng. Med., 9: 931-942.
18. Mhadhbi, M., M. Khitouni, L. Escoda, J.J. Suñol and M. Dammak, 2010. Characterization of mechanically alloyed nanocrystalline Fe(Al): Crystallite size and dislocation density. J. Nanomater., Vol. 2010. 10.1155/2010/712407.
19. Abolghasem, S., S. Basu, S. Shekhar and M.R. Shankar, 2018. Mapping dislocation densities resulting from severe plastic deformation using large strain machining. J. Mater. Res., 33: 3762-3773.
20. Anitha, R., S. Athimoolam, M. Gunasekaran and K. Anitha, 2014. X-ray, vibrational spectra and quantum chemical studies on a new semiorganic crystal: 4-chloroanilinium perchlorate. J. Mol. Struct., 1076: 115-125.
21. H. Tanak, K. Pawlus, M.K. Marchewka, A. Pietraszko 2014. Structural, vibrational and theoretical studies of anilinium trichloroacetate: New hydrogen bonded molecular crystal with nonlinear optical properties. Spectrochim. Acta Part A: Mol. Biomol. Spectrosc., 118: 82-93.
22. Singh, J.S., 2008. FT-IR and raman spectra compared with Ab initio calculated frequency modes for 5-aminouracil. J. Biol. Phys., 34: 569-576.
23. Hadjiivanov, K.I., D.A. Panayotov, M.Y. Mihaylov, E.Z. Ivanova, K.K. Chakarova, S.M. Andonova and N.L. Drenchev, 2021. Power of infrared and raman spectroscopies to characterize metal-organic frameworks and investigate their interaction with guest molecules. Chem. Rev., 121: 1286-1424.
24. Muthuselvi, C., S. Amirthakan and M. Saranya, 2021. Optimization of molecular modeling and spectroscopic studies of 2-acetoxybenzoic acid with 2-hydroxypropane-1,2,3-tricarboxylic acid crystal. Curr. Res. Chem., 13: 15-25.